Detecting the minimum in argon high-harmonic generation spectrum using Gaussian basis sets

Emanuele Coccia, Eleonora Luppi

Theor. Chem. Acc. manuscript No.
(will be inserted by the editor)

Detecting the minimum in argon high-harmonic generation spectrum using Gaussian basis sets

Emanuele Coccia · **Eleonora Luppi**

the date of receipt and acceptance should be inserted later

Abstract Coupling the real-time description of the ultrafast electron dynamics in strong laser fields with quantum chemistry techniques still represents an open challenge for theoreticians. In this work, high-harmonic generation (HHG) spectrum of the argon atom has been computed by means of the time-dependent configuration with singly excited configurations approach (TDCIS), using Gaussian basis sets. We show that adding a number of continuum-optimal Gaussian functions to basis sets routinely used in quantum chemistry calculations, provides the expected position of the intensity minimum in the HHG spectrum, for a given selection of laser intensities and ionisation parameters. Advantages and weaknesses of the proposed computational strategy are discussed. We give evidence here that Gaussian-based TDICS simulations are accurate enough to correctly reproduce the features of ultrafast and highly nonlinear optical processes, as HHG.

Keywords Nonlinear optics · strong fields · ionisation

Electron dynamics in atoms and molecules interacting with an intense and ultrashort laser pulse has becoming an attractive and largely diffused research field since the advent of the attosecond laser pulses [1]. As an example, high-harmonic generation (HHG) [2,3] spectra are successfully used to explain the attosecond dynamics of electronic wave packets [4]. From a theoretical perspective, achieving a robust understanding of the mechanisms controlling the electron dynamics affected by a strong laser field is still a challenge and several approaches have been proposed [4]. One of them is given by the real-time propagation of the electronic wave function expanded in the basis of field-free eigenstates from configuration interaction with singly excited configurations (TDCIS) [5–10], coupled to Gaussian basis sets. Computation of HHG spectrum of atomic and molecular species using standard quantum-chemistry

E. Coccia
Dipartimento di Scienze Chimiche e Farmaceutiche, Università di Trieste, 34127, Trieste (Italy)
E-mail: ecoccia@units.it

E. Luppi
Laboratoire de Chimie Théorique, Sorbonne Université, F-75005, Paris (France)

Table 1 Parameters of the calculations using $I = 10^{14}, 2\times10^{14}$ and 3×10^{14} W/cm^2.

I (W/cm^2)	N_{cutoff}	γ	d_0 (bohr)	d_1 (bohr)
10^{14}	23	1.16	16.5	0.1
2×10^{14}	35	0.82	23	0.1
3×10^{14}	47	0.67	28	0.1

approaches and Gaussian basis sets [11,7–9,12,10,13], "enriched" by a number of optimal Gaussian basis functions for the continuum (called here K) [14,9,12,10,13], has been recently shown as reliable and accurate in the detection of the specific features of the spectrum, as a minimum in the harmonic intensity of H_2^+ HHG spectrum [13]. On the other hand, limitations of Gaussian-based approaches have been pointed out and investigated [9,13].

Argon atom is well known to show a Cooper minimum in the HHG spectrum [15–18], nearly independent on the applied intensity and due to the its electronic structure. Under slightly different experimental conditions, the energy corresponding to the minimum in HHG spectrum has been found to span the range $48-54$ eV [15,17, 19].

Main goal of the present work is the correct description of the minimum in HHG spectrum of argon atom using a TDCIS Gaussian-based representation of the electronic wave packet. It is worth mentioning that our calculations are full-electron, and no approximation (beyond that from choosing the CIS approach) has been made on the way the electronic structure of Ar is represented.

Details on the theoretical and computational strategy have been outlined in the Supporting Information (SI). Our protocol is based on two main ingredients: 1) a field-free CIS calculation using a modified version of Q-Chem package [20,8]; 2) a real-time propagation using the homemade code Light [8,9] to describe electron dynamics interacting with an intense laser field. Time-dependent wave function $|\Psi(t)\rangle$ is expanded in the basis of discrete CIS eigenstates $\{|\psi_k\rangle\}$, $|\Psi(t)\rangle = \sum_k c_k(t)|\psi_k\rangle$, and CIS eigenergies E_k and transition dipole moments $\boldsymbol{\mu}_{kl}$ are used as input parameters for the time propagation (see SI).

Calculations have been carried out by means of two basis sets: 4aug-cc-pVQZ and 4aug-cc-pVQZ+5K, for which 5 K functions for each angular momentum have been included. The net effect of adding 5 K functions is to determine a more "continuous-like" progression of above-threshold state energies (Figure 1 of SI) with respect to the state energies determined by the 4aug-cc-pVQZ basis set, providing a better description of ionisation and recombination steps of the three-step model for HHG [2, 3].

All the calculations have been performed using a laser frequency ω_0 of 1.55 eV ($\lambda_0 = 800$ nm) and a FWHM value of 26 fs (corresponding to 20 optical cycles). A $\cos^2$ envelope function has been adopted (Figure 2 of SI). Laser intensities I (proportional to the square of the field amplitude F_0) of 10^{14}, 2×10 and 3×10^{14} W/cm^2 have been used in our calculations: Keldysh parameter γ [21] is 1.16, 0.82 and 0.67, respectively (Table 1). HHG spectrum is given by the Fourier transform of the time-dependent dipole (Figure 3 of SI). HHG spectra are reported in logarithmic scale.

Computational details on simulations and how K functions are obtained are found in SI.

Double-d heuristic lifetimes model [9,12,10,13] has been used to account for ionisation. Starting from the original model [22], we have split the electron length in two different values, namely d_0 for above-threshold states below $I_p + 3.17U_p$ (with U_p being the ponderomotive energy) and a much smaller d_1 for states above that limit. Values of d_0 and d_1 employed in the simulations are collected in Table 1. The value of d_0 corresponds to the classical quiver amplitude of the highest return F_0/ω_0^2. Such a choice for d_0 follows the related discussion in Ref. [23] on the position of the complex absorbing potential. We found that choosing d_0 and d_1 according to the values collected in Table 1 produces the most accurate description of the high-energy region of HHG spectra, provided the basis set and the laser parameters. Effects of changing d_0 and of using the original heuristic lifetimes model are shown in Figures 4-9 of SI.

As reported elsewhere [9,12,10], a balanced number of diffuse and K functions should be used in a Gaussian basis set suited to accurately represent ultrafast electron dynamics in nonlinear processes. Such a basis set is able to describe Rydberg and above-threshold states (i.e., in our case, $Ar^+ + e^-$), at least in a limited energy and spatial range. Main limitations in the construction of this kind of basis set come from linear dependence issues in the self-consistent field calculations and memory requirements: choosing 4aug-cc-pVQZ+5K therefore represents an interplay between numerical stability, efficiency and physical significance.

Main goal of the present Letter is pointing out the fundamental role played by K functions in the description of the high-energy portion of the HHG spectrum of argon atom and, consequently, of the position of the Cooper minimum: for this reason HHG spectra with and without K functions are reported here for comparison. Figure 1 shows HHG spectra without (panel A) and with (panel B) K functions for a laser intensity $I = 2 \times 10^{14}$ W/cm^2. Low- and intermediate-energy harmonics peaks are well described by both Gaussian basis sets, as well as for the cutoff position (the vertical dot-dashed line indicates the position of the semiclassical three-step model estimate at the 35th harmonic, Table 1): H35 for 4aug-cc-pVQZ and H35-H37 for 4aug-cc-pVQZ+5K (Hn indicates the n-th harmonic in the spectrum). On the other hand, evident differences are seen in the high-energy region (approximately H27-H37): only in presence of K functions, a dip in the intensity and a minimum at around H31 are found. Minimum at H31 ($\sim$ 48 eV) lies in the experimental range 48-54 eV [15,17, 19].

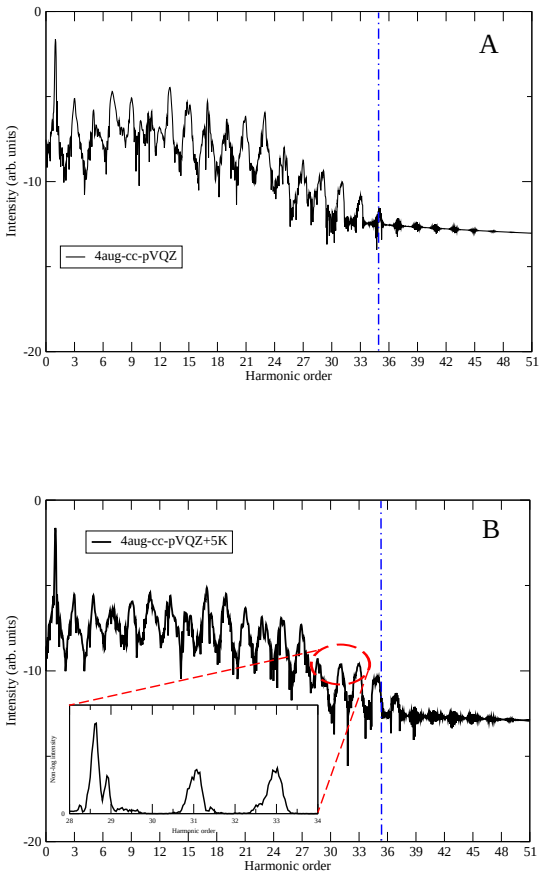

Fig. 1 A: HHG spectrum of the argon atom using $I = 2 \times 10^{14}$ W/cm^2 and $\lambda_0 = 800$ nm with a 4aug-cc-pVQZ basis set. B: the same as for A but with a 4aug-cc-pVQZ+5K basis set. Ionisation is taken into account using $d_0 = 23$ a.u. and $d_1 = 0.1$ a.u.. Inset in panel B shows the non-logarithmic HHG spectrum at minimum.

At lower intensity, $I = 10^{14}$ W/cm^2, the semiclassical cutoff position is at $\sim$ H23, as shown in Figure 2. HHG spectra without (panel A) and with K functions (panel B) show several similarities until H23. In both cases, more harmonics appear at higher energies, indicating a quite poor agreement with the three-step model prediction; however, only 3/4 "extra" harmonics are present when K functions are employed, while using the 4aug-cc-pVQZ basis set produces 7/8 above-cutoff harmonics. Cooper minimum can not be therefore detected with K functions in this case, because the HHG signal is not present anymore at the energies expected for the min-

imum to appear. To detect the minimum, it is therefore mandatory to use higher intensities, as reported in Figures 1 and 3.

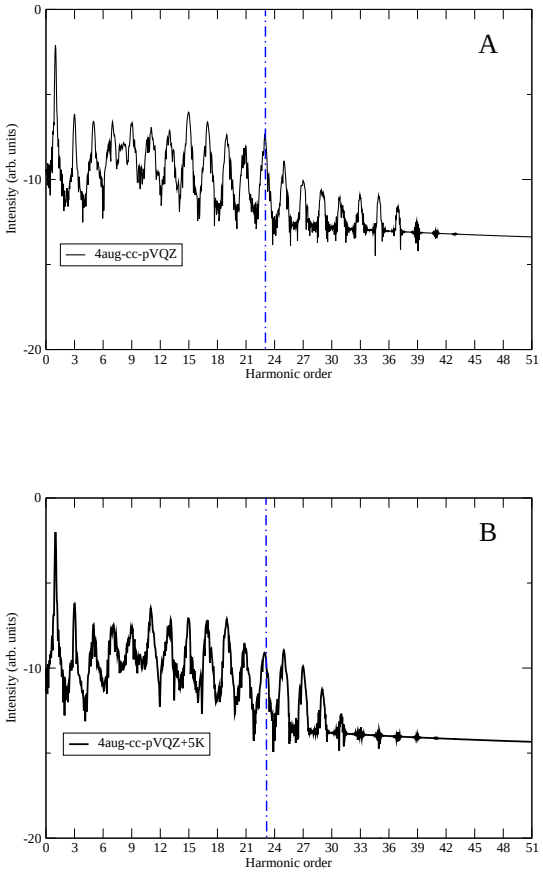

Fig. 2 A: HHG spectrum of the argon atom using $I = 10^{14}$ W/cm^2 and $\lambda_0 = 800$ nm with a 4aug-cc-pVQZ basis set. B: the same as for A but with a 4aug-cc-pVQZ+5K basis set. Ionisation is taken into account using $d_0 = 16.5$ a.u. and $d_1 = 0.1$ a.u..

With an intensity of 3×10^{14} W/cm^2, higher-energy harmonics are produced (Figure 3): using K functions a clear cutoff is seen at H45 (panel B, the semiclassical value is H47), while a set of low-intensity peaks is observed in absence of K functions (panel A). Due to the poor description of above-threshold states with 4aug-cc-pVQZ and to the fact that these states are populated with larger probability by

increasing the laser intensity, the high-energy portion of HHG spectrum in panel A, with $I = 3 \times 10^{14}$ W/cm^2, is likely affected by numerical noise.
A clear minimum is obtained only in presence of K functions (panel B of Figure 3) at H29 (~ 45 eV), in reasonable agreement with the experimental findings[15, 17, 19]. As a general comment, we have already pointed out that the size of the chosen basis set (in terms of both diffuse and K functions) should increase with laser intensity [9]: for this reason, we do not expect to get the same accuracy in the computation of the HHG spectra collected in Figures 1, 2 and 3.

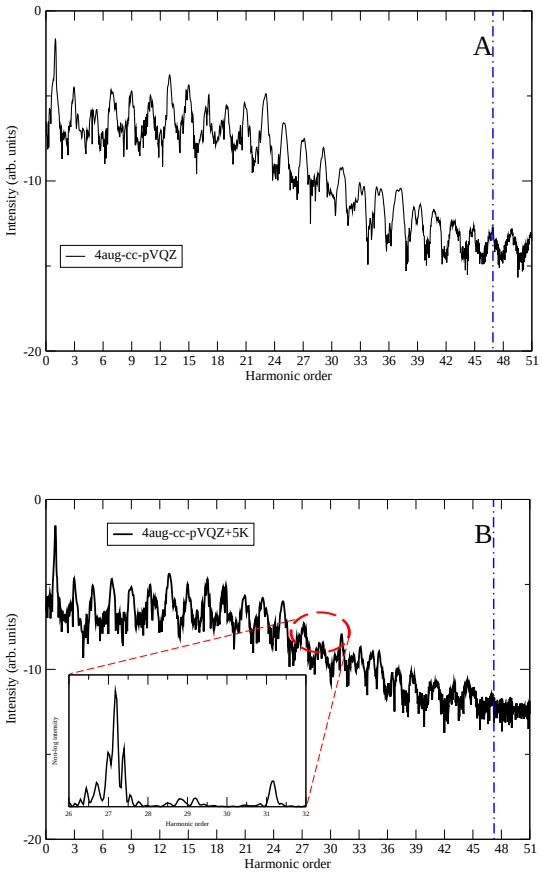

Fig. 3 A: HHG spectrum of the argon atom using $I = 3 \times 10^{14}$ W/cm^2 and $\lambda_0 = 800$ nm with a 4aug-cc-pVQZ basis set. B: the same as for A but with a 4aug-cc-pVQZ+5K basis set. Ionisation is taken into account using $d_0 = 28$ a.u. and $d_1 = 0.1$ a.u.. Inset in panel B shows the non-logarithmic HHG spectrum at minimum.

Including ionisation rates for above-threshold states is necessary for accounting for the incompleteness of the basis. We have verified that the use of the double-d heuristic lifetimes model with the values reported in Table 1 gives the best signal-to-noise ratio to properly detect the Cooper minimum, at the laser conditions employed here. Time-dependent ionisation probability $W(t) = 1 - \sum_{k\in\text{bound}} |c_k(t)|^2$, where k runs on the states below the ionisation threshold, is reported for the two basis sets and the three intensities in Figure 4. $W(t)$ is smaller for 4aug-cc-pVTQZ+5K calculations because of a more precise representation of the above-threshold states.

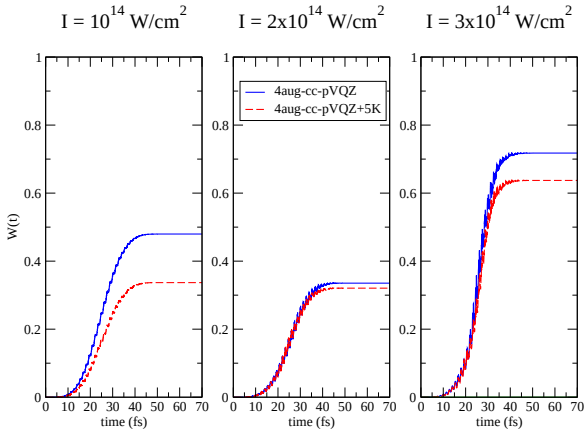

Fig. 4 Ionisation probability $W(t)$ for $I = 10^{14}$, 2×10^{14} and 3×10^{14} W/cm^2 and $\lambda_0 = 800$ nm, using the 4aug-cc-pVQZ and 4aug-cc-pVQZ+5K basis sets. Ionisation parameters are d_0 = 16.5, 23 and 28 a.u. for the three intensities, respectively, and d_1 = 0.1 a.u..

Role of K functions has been seen to be essential to correctly describe and locate the intensity minimum in the HHG spectrum of Ar. Minimum disappears in absence of K functions in the wave function representation. We have propagated the full-electron wave function interacting with very intense laser fields. These results are robust and in agreement with experimental references, within the intensity range investigated in the present work and with the employed ionisation modelling.
Further investigations will provide a deeper insight on the role of electron correlation in the description of HHG spectrum of the argon atom, going beyond the CIS approximation: use of hybrid functionals in real-time TDDFT calculations will allow us to dissect contributions from exchange and correlation to the time evolution of the electron density. Moreover, in order to verify the robustness of the preliminary results presented in this Letter, simulations with different pulse parameters (e.g., frequency and duration) will be carried out.

Acknowledgements Authors thank Piero Decleva and Julien Toulouse for useful discussions. EC acknowledges the Computing Center of the University of Trieste.

Supporting Information

Theoretical and computational details. CIS energy states for 4aug-cc-pVQZ and 4aug-cc-pVQZ+5K (Figure 1). Applied field (Figure 2) and transition dipole moments (Figure 3). HHG spectra and ionisation probability for different choices of the ionisation model and/or of the value of d_0 (Figures 4-9).

References

1. M. Chini, K. Zhao, Z. Chang, Nat. Photonics **8**, 178 (2014)
2. P.B. Corkum, Phys. Rev. Lett. **71**, 1994 (1993)
3. M. Lewenstein, P. Balcou, M.Y. Ivanov, A. L'Huillier, P.B. Corkum, Phys. Rev. A **49**, 2117 (1994)
4. M. Nisoli, P. Decleva, F. Calegari, A. Palacios, F. Martín, Chem. Rev. **117**, 10760 (2017)
5. T. Klamroth, Phys. Rev. B **68**, 245421 (2003)
6. P. Krause, T. Klamroth, P. Saalfrank, J. Chem. Phys. **127**, 034107 (2007)
7. E. Luppi, M. Head-Gordon, Mol. Phys. **110**, 909 (2012)
8. E. Luppi, M. Head-Gordon, J. Chem. Phys. **139**, 164121 (2013)
9. E. Coccia, B. Mussard, M. Labeye, J. Caillat, R. Taieb, J. Toulouse, E. Luppi, Int. J. Quantum Chem. **116**, 1120 (2016)
10. E. Coccia, R. Assaraf, E. Luppi, J. Toulouse, J. Chem. Phys. **147**, 014106 (2017)
11. A. White, C.J. Heide, P. Saalfrank, M. Head-Gordon, E. Luppi, Mol. Phys. **114**, 947 (2016)
12. E. Coccia, E. Luppi, Theor. Chem. Acc. **135**, 43 (2016)
13. M. Labeye, F. Zapata, E. Coccia, V. Véniard, J. Toulouse, J. Caillat, R. Taïeb, E. Luppi, J. Chem. Theory Comput. **14**, 5846 (2018)
14. K. Kaufmann, W. Baumeister, M. Jungen, J. Phys. B **22**, 2223 (1989)
15. S. Minemoto, T. Umegaki, Y. Oguchi, T. Morishita, A.T. Le, S. Watanabe, H. Sakai, Phys. Rev. A **78**, 061402(R) (2008)
16. T. Morishita, A.T. Le, Z. Chen, C.D. Lin, Phys. Rev. Lett. **100**, 013903 (2008)
17. H. J. Wörner and H. Niikura and J. B. Bertrand and P. B. Corkum and D. M. Villeneuve, Phys. Rev. Lett. **102**, 103901 (2009)
18. O. Hassouneh, N.B. Tyndall, J. Wragg, H.W. van der Hart, A.C. Brown, Phys. Rev. A **98**, 043419 (2018)
19. J. Higuet, H. Ruf, N. Thiré, R. Cireasa, E. Constant, E. Cormier, D. Descamps, E. Mével, S. Petit, B. Pons, Y. Mairesse, , B. Fabre, Phys. Rev. A **83**, 053401 (2011)
20. Y. Shao, *et al.* , Mol. Phys. **113**, 184 (2015)
21. L. V. Keldysh, Sov. Phys. JETP, **20**, 1307 (1965)
22. S. Klinkusch, P. Saalfrank, T. Klamroth, J. Chem. Phys. **131**, 114304 (2009)
23. M. Ruberti, P. Decleva, V. Averbukh, Phys. Chem. Chem. Phys. **20**, 8311 (2018)